Drivers of plant nutrient acquisition and allocation strategies and their influence on plant responses to environmental change

by

Evan A. Perkowski, B.S.

A Dissertation

In

Biological Sciences

Submitted to the Graduate Faculty
of Texas Tech University in
Partial Fulfillment of
the Requirements for
the Degree of

Doctor of Philosophy

Approved

Dr. Nicholas G. Smith
Chair of Committee

Dr. Aimée T. Classen

Dr. Natasja van Gestel

Dr. Lindsey C. Slaughter

Dr. Dylan W. Schwilk

Dr. Mark Sheridan
Dean of the Graduate School

May 2023

Acknowledgements

Placeholder for text

Table of Contents

Abstract

List of Tables

List of Figures

1 Chapter 1

2 Introduction

Chapter 2

Structural carbon costs to acquire nitrogen are determined by nitrogen and light availability in two species with different nitrogen acquisition strategies

2.1 Introduction

Carbon and nitrogen cycles are tightly coupled in terrestrial ecosystems. This tight coupling influences photosynthesis (**?**; **?**), net primary productivity (**?**; **?**), decomposition (**?**; **?**; **?**), and plant resource competition (**?**; **?**). Terrestrial biosphere models are beginning to include connected carbon and nitrogen cycles to improve the realism of their simulations (**?**; **?**; **?**; **?**; **?**). Simulations from these models indicate that coupling carbon and nitrogen cycles can drastically influence future biosphere-atmosphere feedbacks under global change, such as elevated carbon dioxide or nitrogen deposition (**?**; **?**; **?**; **?**). Nonetheless, there are still limitations in our quantitative understanding of connected carbon and nitrogen dynamics (**?**; **?**; **?**; **?**; **?**), forcing models to make potentially unreliable assumptions.

Plant nitrogen acquisition is a process in terrestrial ecosystems by which carbon and nitrogen are tightly coupled (**?**; **?**; **?**). Plants must allocate photosynthetically derived carbon belowground to produce and maintain root systems or exchange with symbiotic soil microbes in order to acquire nitrogen (**?**; **?**). Thus, plants have an inherent carbon cost associated with acquiring nitrogen, which can include both direct energetic costs associated with nitrogen acquisition and indirect costs associated with building structures that support nitrogen acquisition (**?**; **?**; **?**; **?**). Model simulations (**?**; **?**; **?**; **?**) and meta-analyses (**?**) suggest that

these carbon costs vary between species, particularly those with different nitrogen acquisition strategies. For example, simulations using iterations of the Fixation and Uptake of Nitrogen (FUN) model indicate that species that acquire nitrogen from non-symbiotic active uptake pathways (e.g. mass flow) generally have larger carbon costs to acquire nitrogen than species that acquire nitrogen through symbiotic associations with nitrogen-fixing bacteria (**?**; **?**).

Carbon costs to acquire nitrogen likely vary in response to changes in soil nitrogen availability. For example, if the primary mode of nitrogen acquisition is through non-symbiotic active uptake, then nitrogen availability could decrease carbon costs to acquire nitrogen as a result of increased per-root nitrogen uptake (**?**; **?**). However, if the primary mode of nitrogen acquisition is through symbiotic active uptake, then nitrogen availability may incur additional carbon costs to acquire nitrogen if it causes microbial symbionts to shift toward parasitism along the parasitism–mutualism continuum (**?**; **?**; **?**) or if it reduces the nitrogen acquisition capacity of a microbial symbiont (**?**; **?**; **?**). Species may respond to shifts in soil nitrogen availability by switching their primary mode of nitrogen acquisition to a strategy with lower carbon costs to acquire nitrogen in order to maximize the magnitude of nitrogen acquired from a belowground carbon investment and outcompete other individuals for soil resources (**?**; **?**).

Environmental conditions that affect demand to acquire nitrogen to support new and existing tissues could also be a source of variance in plant carbon costs to acquire nitrogen. For example, an increase in plant nitrogen demand could increase carbon costs to acquire nitrogen if this increases the carbon that must be allocated belowground to acquire a proportional amount of nitrogen (**?**;

?). This could be driven by a temporary state of diminishing return associated with investing carbon toward building and maintaining structures that are necessary to support enhanced nitrogen uptake, such as fine roots (?; ?; ?), mycorrhizal hyphae (?), or root nodules (?). Alternatively, if the environmental factor that increases plant nitrogen demand causes nitrogen to become more limiting in the system (e.g. atmospheric CO2; ?, ?, ?, ?), species might switch their primary mode of nitrogen acquisition to a strategy with lower relative carbon costs to acquire nitrogen in order to gain a competitive advantage over species with either different or more limited modes of nitrogen acquisition (?; ?).

Using a plant economics approach, we examined the influence of plant nitrogen demand and soil nitrogen availability on plant carbon costs to acquire nitrogen. This was done by growing a species capable of forming associations with nitrogen-fixing bacteria (*Glycine max* L. (Merr)) and a species not capable of forming these associations (*Gossypium hirsutum* L.) under four levels of light availability (plant nitrogen demand proxy) and four levels of soil nitrogen fertilization (soil nitrogen availability proxy) in a full-factorial, controlled greenhouse experiment. We used this experimental set-up to test the following hypotheses:

1. An increase in plant nitrogen demand due to increasing light availability will increase carbon costs to acquire nitrogen through a proportionally larger increase in belowground carbon than whole-plant nitrogen acquisition. This will be the result of an increased investment of carbon toward belowground structures that support enhanced nitrogen uptake, but at a lower nitrogen return.

2. An increase in soil nitrogen availability will decrease carbon costs to acquire

nitrogen as a result of increased per root nitrogen uptake in *G. hirsutum*. However, soil nitrogen availability will not affect carbon costs to acquire nitrogen in *G. max* because of the already high return of nitrogen supplied through nitrogen fixation.

2.2 Methods

2.2.1 *Experiment setup*

Gossypium hirsutum and *G. max* were planted in individual 3 liter pots (NS-300; Nursery Supplies, Orange, CA, USA) containing a 3:1 mix of unfertilized potting mix (Sungro Sunshine Mix #2, Agawam, MA, USA) to native soil extracted from an agricultural field most recently planted with *G. max* at the USDA-ARS Laboratory in Lubbock, TX, USA (33.59°N, –101.90°W). The field soil was classified as Amarillo fine sandy loam (75% sand, 10% silt, 15% clay). Upon planting, all *G. max* pots were inoculated with *Bradyrhizobium japonicum* (Verdesian N-Dure™ Soybean, Cary, NC, USA) to stimulate root nodulation. Individuals of both species were grown under similar, unshaded, ambient greenhouse conditions for 2 weeks to germinate and begin vegetative growth. Three blocks were set up in the greenhouse, each containing four light treatments created using shade cloth that reduced incoming radiation by either 0 (full sun), 30, 50, or 80%. Two weeks post-germination, individuals were randomly placed in the four light treatments in each block. Individuals received one of four nitrogen fertilization doses as 100ml of a modified Hoagland solution (**?**) equivalent to either 0, 70, 210, or 630 ppm N twice per week within each light treatment. Nitrogen fertilization doses were received as topical agents to the soil surface. Each Hoagland solution

was modified to keep concentrations of other macro- and micronutrients equivalent (Supplementary Table S1). Plants were routinely well watered to eliminate water stress.

2.2.2 *Plant measurements and calculations*

Each individual was harvested after 5 weeks of treatment, and biomass was separated by organ type (leaves, stems, and roots). Nodules on *G. max* roots were also harvested. With the exception of the 0% shade cover and 630 ppm N treatment combination, all treatment combinations in both species had lower average dry biomass:pot volume ratios than the 1:1 ratio recommended by **?** to minimize the likelihood of pot volume-induced growth limitation (Supplementary Tables S2, S3; Supplementary Fig. S1). All harvested material was dried, weighed, and ground by organ type. Carbon and nitrogen content (g g^{-1}) was determined by subsampling from ground and homogenized biomass of each organ type using an elemental analyzer (Costech 4010; Costech, Inc., Valencia, CA, USA). We scaled these values to total leaf, stem, and root carbon and nitrogen biomass (g) by multiplying dry biomass of each organ type by carbon or nitrogen content of each corresponding organ type. Whole-plant nitrogen biomass (g) was calculated as the sum of total leaf (g), stem (g), and root (g) nitrogen biomass. Root nodule carbon biomass was not included in the calculation of root carbon biomass; however, relative plant investment toward root or root nodule standing stock was estimated as the ratio of root biomass to root nodule biomass (g g^{-1}), following similar metrics to those adopted by **?** and **?**.

Carbon costs to acquire nitrogen (gC gN^{-1}) were estimated as the ratio of

total root carbon biomass (gC) to whole-plant nitrogen biomass (gN). This calculation quantifies the relationship between carbon spent on nitrogen acquisition and whole-plant nitrogen acquisition by using root carbon biomass as a proxy for estimating the magnitude of carbon allocated toward nitrogen acquisition. This calculation therefore assumes that the magnitude of root carbon standing stock is proportional to carbon transferred to root nodules or mycorrhizae, or lost through root exudation or turnover. This assumption has been supported in species that associate with ectomycorrhizal fungi (**?**; **?**), but is less clear in species that acquire nitrogen through non-symbiotic active uptake or symbiotic nitrogen fixation. It is also unclear whether relationships between root carbon standing stock and carbon transfer to root nodules are similar in magnitude to carbon lost through exudation or when allocated toward other active uptake pathways. Thus, because of the way we performed our measurements, our proximal values of carbon costs to acquire nitrogen are underestimates.

2.2.3 *Statistical analyses*

We explored the effects of light and nitrogen availability on carbon costs to acquire nitrogen using separate linear mixed-effects models for each species. Models included shade cover, nitrogen fertilization, and interactions between shade cover and nitrogen fertilization as continuous fixed effects, and also included block as a random intercept term. Three separate models for each species were built with this independent variable structure for three different dependent variables: (i) carbon costs to acquire nitrogen (gC gN^{-1}); (ii) whole-plant nitrogen biomass (denominator of carbon cost to acquire nitrogen; gN); and (iii) root carbon biomass

(numerator of carbon cost to acquire nitrogen; gC). We constructed two additional models for *G. max* with the same model structure described above to investigate the effects of light availability and nitrogen fertilization on root nodule biomass (g) and the ratio of root nodule biomass to root biomass (unitless).

We used Shapiro–Wilk tests of normality to determine whether species-specifc linear mixed-effects model residuals followed a normal distribution. None of our models satisfied residual normality assumptions when models were fit using untransformed data (Shapiro–Wilk: $P<0.05$ in all cases). We attempted to satisfy residual normality assumptions by first fitting models using dependent variables that were natural-log transformed. If residual normality assumptions were still not met (Shapiro–Wilk: $P<0.05$), then models were fit using dependent variables that were square root transformed. All residual normality assumptions were satisfied when models were fit with either a natural-log or square root transformation (Shapiro–Wilk: $P>0.05$ in all cases). Specifically, we natural-log transformed *G. hirsutum* carbon costs to acquire nitrogen and *G. hirsutum* whole-plant nitrogen biomass. We also square root transformed *G. max* carbon costs to acquire nitrogen, *G. max* whole-plant nitrogen biomass, root carbon biomass in both species, *G. max* root nodule biomass, and the *G. max* ratio of root nodule biomass to root biomass. We used the 'lmer' function in the 'lme4' R package (**?**) to fit each model and the 'Anova' function in the 'car' R package (**?**) to calculate Wald's χ^2 to determine the significance (α=0.05) of each fixed effect coefficient. Finally, we used the 'emmeans' R package (**?**) to conduct post-hoc comparisons of our treatment combinations using Tukey's tests. Degrees of freedom for all Tukey's tests were approximated using the Kenward–Roger approach (**?**). All analyses

and plots were conducted in R version 4.0.1 (**?**).

2.3 Results

2.3.1 *Carbon costs to acquire nitrogen*

Carbon costs to acquire nitrogen in *G. hirsutum* increased with increasing light availability (P<0.001; Table 1; Fig. 1) and decreased with increasing nitrogen fertilization (P<0.001; Table 1; Fig. 1). There was no interaction between light availability and nitrogen fertilization (P=0.486; Table 2.1; Fig. 2.1).

Carbon costs to acquire nitrogen in *G. max* also increased with increasing light availability (P<0.001; Table 1; Fig. 1) and decreased with increasing nitrogen fertilization (P<0.001; Table 1; Fig. 1). There was no interaction between light availability and nitrogen fertilization (P=0.261; Table 2.1; Fig. 2.1).

Table 2.1. Analysis of variance results exploring species-specific effects of light availability, nitrogen fertilization, and their interactions on carbon costs to acquire nitrogen, whole-plant nitrogen biomass, and root carbon biomass

		Carbon costs to acquire nitrogen			Whole-plant nitrogen biomass			Root carbon biomass		
	df	Coefficient	χ^2	*P*-value	Coefficient	χ^2	*P*-value	Coefficient	χ^2	*P*-value
G. hirsutum										
Intercept		1.594	-	-	-3.232	-	-	0.432	-	-
Light (L)	1	-1.09E-02	56.494	**<0.001**	-6.41E-03	91.275	**<0.001**	-2.62E-03	169.608	**<0.001**
Nitrogen (N)	1	-1.34E-03	54.925	**<0.001**	1.83E-03	118.784	**<0.001**	1.15E-04	2.901	*0.089*
L*N	1	3.88E-06	0.485	0.486	-1.34E-05	10.721	**0.001**	-1.67E-06	3.140	*0.076*
G. max										
Intercept		1.877	-	-	0.239	-	-	0.438	-	-
Light (L)	1	-7.67E-03	174.156	**<0.001**	-6.72E-04	39.799	**<0.001**	-2.55E-03	194.548	**<0.001**
Nitrogen (N)	1	-2.35E-04	21.948	**<0.001**	1.55E-04	70.771	**<0.001**	2.52E-04	19.458	**<0.001**
L*N	1	-2.89E-06	1.262	0.261	-6.32E-07	1.435	0.231	-3.16E-06	10.803	**0.001**

*Significance determined using Wald's χ^2 tests (P=0.05). P-values<0.05 are in bold and marginally insignificant P-values between 0.050 and 0.100 are italicized. Negative coefficients for light treatments indicate a positive effect of increasing light availability on all response variables, as light availability is treated as percent shade cover in all linear mixed-effects models.

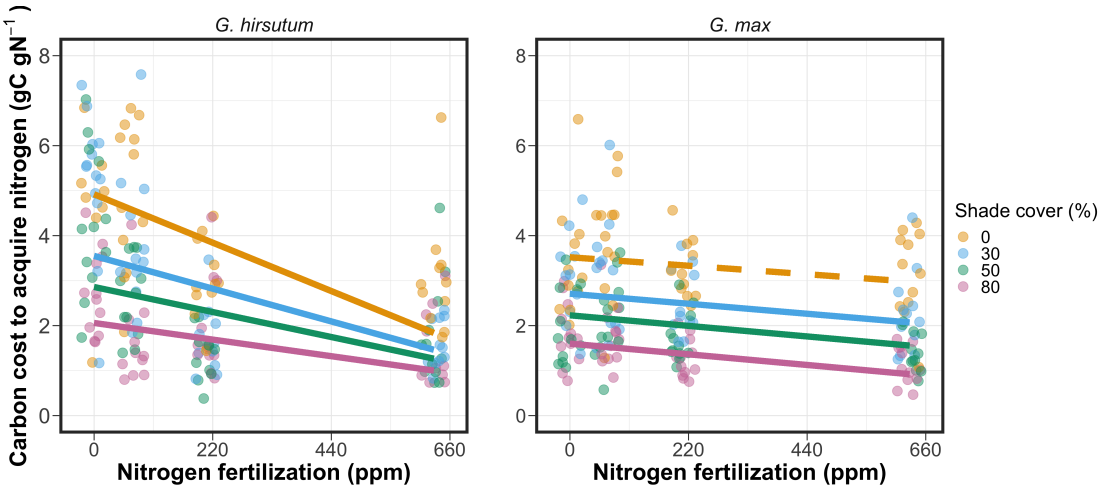

Figure 2.1. Relationships between soil nutrient fertilization and light availability on carbon costs to acquire nitrogen in *G. hirsutum* and *G. max*. Nitrogen fertilization treatments are represented on the x-axis. Shade cover treatments are represented through colored points and trendlines. Trendlines were created by back-transforming marginal mean slopes and intercepts from species-specific linear mixed-effects models. These values were calculated using the 'emtrends' and 'emmeans' functions in the 'emmeans' R package (Lenth, 2019). Points are jittered for visibility. Yellow points and trendlines represent the 0% shade cover treatment, blue points and trendlines represent the 30% shade cover treatment, green points and trendlines represent the 50% shade cover treatment, and purple points and trendlines represent the 80% shade cover treatment. Solid trendlines indicate slopes that are significantly different from zero (Tukey: $P<0.05$), while dashed trendlines indicate slopes that are not statistically different from zero.

2.3.2 *Whole plant nitrogen biomass*

Whole-plant nitrogen biomass in *G. hirsutum* was driven by an interaction between light availability and nitrogen fertilization (P=0.001; Table 1; Fig. 2). This interaction indicated a greater stimulation of whole-plant nitrogen biomass by nitrogen fertilization as light levels increased (Table 2.1; Fig. 2.2).

Whole-plant nitrogen biomass in *G. max* increased with increasing light availability (P<0.001) and nitrogen fertilization (P<0.001), with no interaction between light availability and nitrogen fertilization (P=0.231; Table 2.1; Fig. 2.2).

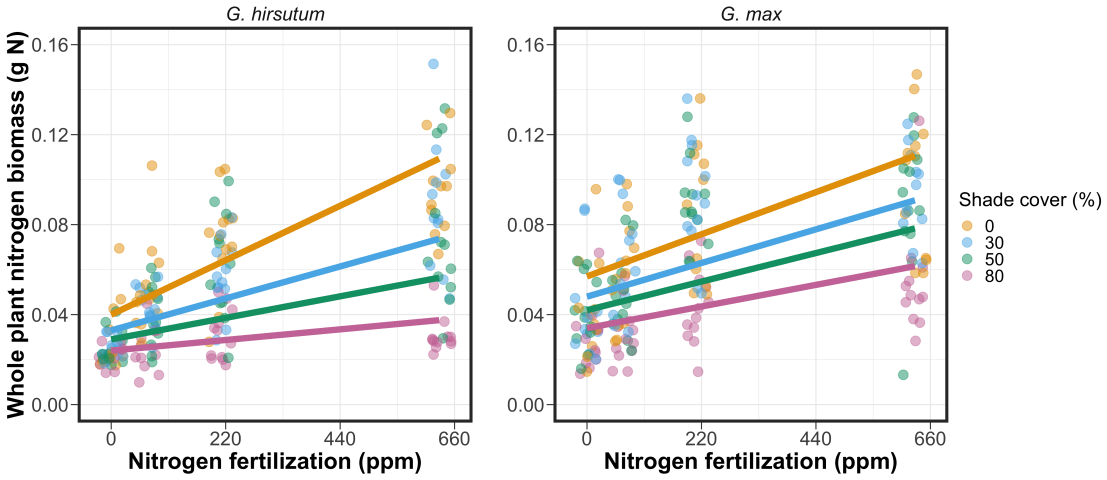

Figure 2.2. Relationships between soil nutrient fertilization and light availability on whole-plant nitrogen biomass in *G. hirsutum* and *G. max*.Whole-plant nitrogen biomass is the denominator of the carbon cost to acquire nitrogen calculation. Nitrogen fertilization treatments are represented on the x-axis. Shade cover treatments are represented through colored points and trendlines. Trendlines were created by back-transforming marginal mean slopes and intercepts from species-specific linear mixed-effects models. These values were calculated using the 'emtrends' and 'emmeans' functions in the 'emmeans' R package (**?**). Points are jittered for visibility. Yellow points and trendlines represent the 0% shade cover treatment, blue points and trendlines represent the 30% shade cover treatment, green points and trendlines represent the 50% shade cover treatment, and purple points and trendlines represent the 80% shade cover treatment. Solid trendlines indicate slopes that are significantly different from zero (Tukey: $P<0.05$), while dashed trendlines indicate slopes that are not statistically different from zero.

2.3.3 *Root carbon biomass*

Root carbon biomass in *G. hirsutum* significantly increased with increasing light availability (P<0.001; Table 1; Fig. 3) and marginally increased with nitrogen fertilization (P=0.089; Table 1; Fig. 3). There was also a marginal interaction between light availability and nitrogen fertilization (P=0.076; Table 1), driven by an increase in the positive response of root carbon biomass to increasing nitrogen fertilization as light availability increased. This resulted in significantly positive trends between root carbon biomass and nitrogen fertilization in the two highest light treatments (Tukey: P<0.05 in both cases; Table 2.3; Fig. 2.3) and no effect of nitrogen fertilization in the two lowest light treatments (Tukey: P>0.05 in both cases; Table 3; Fig. 3).

There was an interaction between light availability and nitrogen fertilization on root carbon biomass in *G. max* (P=0.001; Table 1; Fig. 3). Post-hoc analyses indicated that the positive effects of nitrogen fertilization on G.! max root carbon biomass increased with increasing light availability (Table 3; Fig. 3). There were also positive individual effects of increasing nitrogen fertilization (P<0.001) and light availability (P<0.001) on *G. max* root carbon biomass (Table 1; Fig. 2.3).

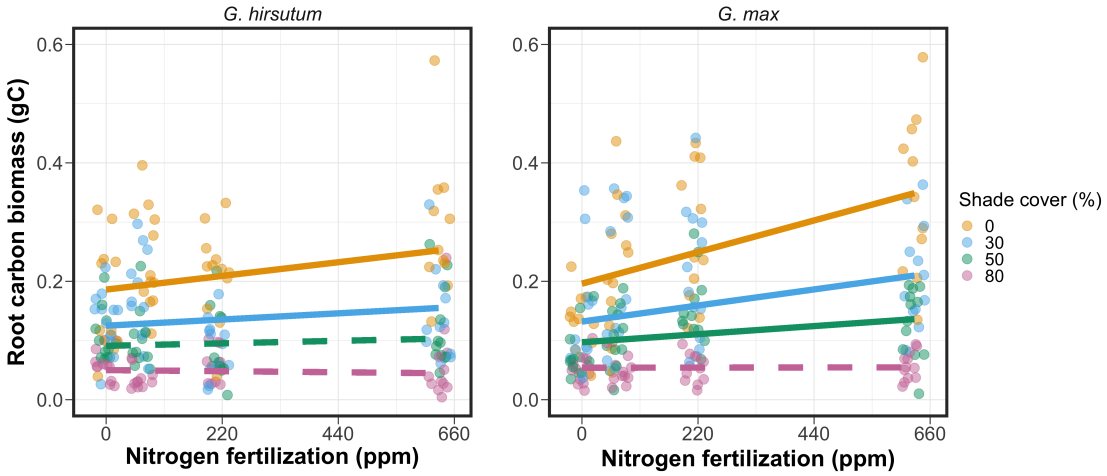

Figure 2.3. Relationships between soil nutrient fertilization and light availability on root carbon biomass in *G. hirsutum* and *G. max*. Root carbon biomass is the numerator of the carbon cost to acquire nitrogen calculation. Nitrogen fertilization treatments are represented on the x-axis. Shade cover treatments are represented through colored points and trendlines. Trendlines were created by back-transforming marginal mean slopes and intercepts from species-specific linear mixed-effects models. These values were calculated using the 'emtrends' and 'emmeans' functions in the 'emmeans' R package (**?**). Points are jittered for visibility. Yellow points and trendlines represent the 0% shade cover treatment, blue points and trendlines represent the 30% shade cover treatment, green points and trendlines represent the 50% shade cover treatment, and purple points and trendlines represent the 80% shade cover treatment. Solid trendlines indicate slopes that are significantly different from zero (Tukey: $P<0.05$), while dashed trendlines indicate slopes that are not statistically different from zero.

2.3.4 *Root nodule biomass*

Root nodule biomass in *G. max* increased with increasing light availability (P<0.001; Table 2; Fig. 4A) and decreased with increasing nitrogen fertilization (P<0.001; Table 2; Fig. 4A). There was no interaction between nitrogen fertilization and light availability (P=0.133; Table 2; Fig. 4A). The ratio of root nodule biomass to root biomass did not change in response to light availability (P=0.481; Table 2; Fig. 4B) but decreased with increasing nitrogen fertilization (P<0.001; Table 2; Fig. 4B). There was no interaction between nitrogen fertilization and light availability on the ratio of root nodule biomass to root biomass (P=0.621; Table 2; Fig. 4B).

Table 2.2. Analysis of variance results exploring effects of light availability, nitrogen fertilization, and their interactions on *G. max* root nodule biomass and the ratio of root nodule biomass to root biomass*

		Nodule biomass			Nodule biomass: root biomass		
	df	Coefficient	χ^2	*P*-value	Coefficient	χ^2	*P*-value
Intercept		0.302	-	-	0.448	-	-
Light (L)	1	-1.81E-03	72.964	**<0.001**	-8.76E-05	0.496	0.481
Nitrogen (N)	1	-2.83E-04	115.377	**<0.001**	-5.09E-04	156.476	**<0.001**
L*N	1	1.14E-06	2.226	0.133	-7.30E-07	0.244	0.621

*Significance determined using Wald's χ^2 tests (α=0.05). *P*-values less than 0.05 are in bold. Negative coefficients for light treatments indicate a positive effect of increasing light availability on all response variables, as light availability is treated as percent shade cover in all linear mixed-effects models. Root nodule biomass and nodule biomass: root biomass models were only constructed for G. max because *G. hirsutum* was not inoculated with *B. japonicum* and is not capable of forming root nodules.

Table 2.3. Slopes of the regression line describing the relationship between each dependent variable and nitrogen fertilization at each light level*

Shade cover	Carbon cost to acquire nitrogen	Whole-plant nitrogen biomass	Root carbon biomass	Root nodule biomass	Nodule biomass root biomass
G. hirsutum					
0%	**-1.34E-03[a]**	**1.83E-03[a]**	**1.15E-04[b]**	-	-
30%	**-1.22E-03[a]**	**1.43E-03[a]**	**1.17E-04[b]**	-	-
50%	**-1.14E-03[a]**	**1.17E-03[a]**	3.12E-05[b]	-	-
80%	**-1.02E-03[a]**	**7.66E-04[a]**	-1.89E-06[b]	-	-
G. max					
0%	-2.35E-04[b]	**1.55E-05[b]**	**2.51E-04[b]**	**-2.83E-04[b]**	**-5.09E-04[b]**
30%	**-3.22E-04[b]**	**1.35E-05[b]**	**1.57E-04[b]**	**-2.49E-04[b]**	**-5.31E-04[b]**
50%	**-3.80E-04[b]**	**1.23E-05[b]**	**9.37E-05[b]**	**-2.26E-04[b]**	**-5.45E-04[b]**
80%	**-4.66E-04[b]**	**1.04E-05[b]**	-9.95E-07[b]	**-1.92E-04[b]**	**-5.67E-04[b]**

*Slopes represent estimated marginal mean slopes from linear mixed-effects models described in the Methods. Slopes were calculated using the 'emmeans' R package (**?**). Superscripts indicate slopes fit to natural-log ([a]) or square root ([b]) transformed data. Slopes statistically different from zero (Tukey: $P<0.05$) are indicated in bold. Marginally significant slopes (Tukey: $0.05<P<0.1$) are italicized.

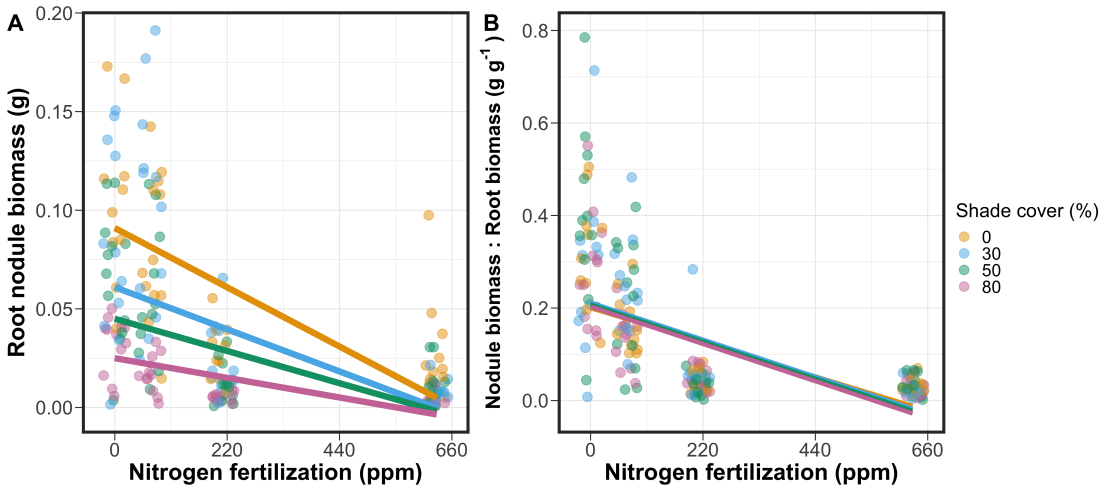

Figure 2.4. Effects of shade cover and nitrogen fertilization on root nodule biomass (A) and the ratio of root nodule biomass to root biomass (B) in *G. max*. Nitrogen fertilization treatments are represented on the x-axis. Shade cover treatments are represented through colored points and trendlines. Trendlines were created by back-transforming marginal mean slopes and intercepts from species-specific linear mixed-effects models. These values were calculated using the 'emtrends' and 'emmeans' functions in the 'emmeans' R package (Lenth, 2019). Points are jittered for visibility. Yellow points and trendlines represent the 0% shade cover treatment, blue points and trendlines represent the 30% shade cover treatment, green points and trendlines represent the 50% shade cover treatment, and purple points and trendlines represent the 80% shade cover treatment. Solid trendlines indicate slopes that are significantly different from zero (Tukey: $P<0.05$), while dashed trendlines indicate slopes that are not statistically different from zero.

2.4 Discussion

In this chapter, we determined the effects of light availability and soil nitrogen fertilization on root mass carbon costs to acquire nitrogen in *G. hirsutum* and *G. max*. In support of our hypotheses, we found that carbon costs to acquire nitrogen generally increased with increasing light availability and decreased with increasing soil nitrogen fertilization in both species. These findings suggest that carbon costs to acquire nitrogen are determined by factors that influence plant nitrogen demand and soil nitrogen availability. In contrast to our second hypothesis, root nodulation data suggested that *G. max* and *G. hirsutum* achieved similar directional carbon cost responses to nitrogen fertilization despite a likely shift in G.!max allocation from nodulation to root biomass along the nitrogen fertilization gradient (Fig. 2.4B).

Both *G. max* and *G. hirsutum* experienced an increase in carbon costs to acquire nitrogen due to increasing light availability. These patterns were driven by a larger increase in root carbon biomass than whole-plant nitrogen biomass. Increases in root carbon biomass due to factors that increase plant nitrogen demand are a commonly observed pattern, as carbon allocated belowground provides substrate needed to produce and maintain structures that satisfy aboveground plant nitrogen demand (**?**; **?**; **?**). Our findings suggest that plants allocate relatively more carbon for acquiring nitrogen when demand increases over short temporal scales, which may cause a temporary state of diminishing return due to asynchrony between belowground carbon and whole-plant nitrogen responses to plant nitrogen demand (**?**; **?**). These responses might be attributed to a temporal lag associated with producing structures that enhance nitrogen acquisition. For ex-

ample, fine roots (**?**; **?**; **?**) and root nodules (**?**) take time to build and first require the construction of coarse roots. Thus, full nitrogen returns from these investments may not occur immediately (**?**; **?**), and may vary by species acquisition strategy. We speculate that increases in nitrogen acquisition from a given carbon investment may occur beyond the 5 week scope of this experiment. A similar study conducted over a longer temporal scale would address this.

Increasing soil nitrogen fertilization generally decreased carbon costs to acquire nitrogen in both species. These patterns were driven by a larger increase in whole-plant nitrogen biomass than root carbon biomass. In *G. hirsutum*, reductions in carbon costs to acquire nitrogen may have been due to an increase in per-root nitrogen uptake, allowing individuals to maximize the amount of nitrogen acquired from a belowground carbon investment. Interestingly, increased soil nitrogen fertilization increased whole-plant nitrogen biomass in *G. max* despite reductions in root nodule biomass that likely reduced the nitrogen-fixing capacity of *G. max* (**?**; **?**). While reductions in root nodulation due to increased soil nitrogen availability are commonly observed (**?**; **?**), our responses were observed in tandem with increased root carbon biomass, implying that *G. max* shifted relative carbon allocation from nitrogen fixation to soil nitrogen acquisition (**?**; **?**). This was likely because there was a reduction in the carbon cost advantage of acquiring fixed nitrogen relative to soil nitrogen, and suggests that species capable of associating with symbiotic nitrogen-fixing bacteria shift their relative nitrogen acquisition pathway to optimize nitrogen uptake (**?**). Future studies should further investigate these patterns with a larger quantity of phylogenetically related species, or different varieties of a single species that differ in their ability to

form associations with symbiotic nitrogen-fixing bacteria to more directly test the impact of nitrogen fixation on the patterns observed in this study.

Carbon costs to acquire nitrogen are subsumed in the general discussion of economic analogies to plant resource uptake (**?**; **?**; **?**; **?**; **?**; **?**). Despite this, terrestrial biosphere models rarely include these carbon costs within their framework for predicting plant nitrogen uptake. There is currently one plant resource uptake model, FUN, that quantitatively predicts carbon costs to acquire nitrogen within a framework for predicting plant nitrogen uptake for different nitrogen acquisition strategies (**?**; **?**). Iterations of FUN are currently coupled to two terrestrial biosphere models: the Community Land Model 5.0 and the Joint UK Land Environment Simulator (**?**; **?**; **?**). Recent work suggests that coupling FUN to CLM 5.0 caused a large overprediction of plant nitrogen uptake associated with nitrogen fixation (**?**). Thus, empirical data from manipulative experiments that explicitly quantify carbon costs to acquire nitrogen in species capable of associating with nitrogen-fixing bacteria across different environmental contexts is an important step toward identifying potential biases in models such as FUN.

Our findings broadly support the FUN formulation of carbon costs to acquire nitrogen in response to soil nitrogen availability. FUN calculates carbon costs to acquire nitrogen based on the sum of carbon costs to acquire nitrogen via nitrogen fixation, mycorrhizal active uptake, non-mycorrhizal active uptake, and retranslocation (**?**; **?**). Carbon costs to acquire nitrogen via mycorrhizal or non-mycorrhizal active uptake pathways are derived as a function of nitrogen availability, root biomass, and two parameterized values based on nitrogen acquisition strategy (**?**). Due to this, FUN simulates a net decrease in carbon costs to acquire

nitrogen with increasing nitrogen availability for mycorrhizal and non-mycorrhizal active uptake pathways, assuming constant root biomass. This was a pattern we observed in *G. hirsutum* regardless of light availability. In contrast, FUN would not simulate a net change in carbon costs to acquire nitrogen via nitrogen fixation due to nitrogen availability. This is because carbon costs to acquire nitrogen via nitrogen fixation are derived from a well-established function of soil temperature, which is independent of soil nitrogen availability (**?**; **?**). We observed a net reduction in carbon costs to acquire nitrogen in *G. max*, except when individuals were grown under 0% shade cover (Fig. 1). While a net reduction of carbon costs in response to nitrogen fertilization runs counter to nitrogen fixation carbon costs simulated by FUN, these patterns were likely because *G. max* individuals switched their primary mode of nitrogen acquisition from symbiotic nitrogen fixation to a non-symbiotic active uptake pathway (Fig. 4B).

It should be noted that the metric used in this study to determine carbon costs to acquire nitrogen has several limitations. Most notably, this metric uses root carbon biomass as a proxy for estimating the amount of carbon spent on nitrogen acquisition. While it is true that most carbon allocated belowground has at least an indirect structural role in acquiring soil resources, it remains unclear whether this assumption holds true for species that acquire nitrogen via symbiotic nitrogen fixation. We also cannot quantify carbon lost through root exudates or root turnover, which may increase due to factors that increase plant nitrogen demand (**?**; **?**), and can increase the magnitude of available nitrogen from soil organic matter through priming effects on soil microbial communities (**?**; **?**). It is also not clear whether these assumptions hold under all environmental conditions,

such as those that shift belowground carbon allocation toward a different mode of nitrogen acquisition (**?**; **?**) or between species with different acquisition strategies. In this study, increasing soil nitrogen fertilization increased carbon investment to roots relative to carbon transferred to root nodules (Fig. 4B). By assuming that carbon allocated to root carbon was proportional to carbon allocated to root nodules across all treatment combinations, these observed responses to soil nitrogen fertilization were likely to be overestimated in *G. max*. We encourage future research to quantify these carbon fates independently.

Researchers conducting pot experiments must carefully choose pot volume to minimize the likelihood of pot volume-induced growth limitation (**?**). **?** indicate that researchers are likely to avoid growth limitations associated with pot volume if measurements are collected when the plant biomass:pot volume ratio is less than 1 g L^{-1}. In this experiment, all treatment combinations in both species had biomass:pot volume ratios less than 1 g L^{-1} except for *G. max* and *G. hirsutum* that were grown under 0% shade cover and had received 630 ppm N. Specifically, *G. max* and *G. hirsutum* had average respective biomass:pot volume ratios of 1.24±0.07g L^{-1} and 1.34±0.13 g L^{-1}, when grown under 0% shade cover and received 630 ppm N (Supplementary Tables S2, S3; Supplementary Fig. S1). If growth in this treatment combination was limited by pot volume, then individuals may have had larger carbon costs to acquire nitrogen than would be expected if they were grown in larger pots. This pot volume induced growth limitation could cause a reduction in per-root nitrogen uptake associated with more densely packed roots, which could reduce the positive effect of nitrogen fertilization on whole-plant nitrogen biomass relative to root carbon biomass (**?**).

Growth limitation associated with pot volume provides a possible explanation for the marginally insignificant effect of increasing nitrogen fertilization on *G. max* carbon costs to acquire nitrogen when grown under 0% shade cover (Table 3; Fig. 1). This is because the regression line describing the relationship between carbon costs to acquire nitrogen and nitrogen fertilization in *G. max* grown under 0% shade cover would have flattened if growth limitation had caused larger than expected carbon costs to acquire nitrogen in the 0% shade cover, 630 ppm N treatment combination. This may have been exacerbated by the fact that *G. max* likely shifted relative carbon allocation from nitrogen fixation to soil nitrogen acquisition, which could have increased the negative effect of more densely packed roots on nitrogen uptake. These patterns could have also occurred in *G. hirsutum* grown under 0% shade cover; however, there was no change in the effect of nitrogen fertilization on *G. hirsutum* carbon costs to acquire nitrogen grown under 0% shade cover relative to other shade cover treatments. Regardless, the possibility of growth limitation due to pot volume suggests that effects of increasing nitrogen fertilization on carbon costs to acquire nitrogen in both species grown under 0% shade cover could have been underestimated. Follow-up studies using a similar experimental design with a larger pot volume would be necessary in order to determine whether these patterns were impacted by pot volume-induced growth limitation.

In conclusion, this study provides empirical evidence that carbon costs to acquire nitrogen are influenced by light availability and soil nitrogen fertilization in a species capable of acquiring nitrogen via symbiotic nitrogen fixation and a species not capable of forming such associations. We show that carbon costs to

acquire nitrogen generally increase with increasing light availability and decrease with increasing nitrogen fertilization. This study provides important empirical data needed to evaluate the formulation of carbon costs to acquire nitrogen in terrestrial biosphere models, particularly carbon costs to acquire nitrogen that are associated with symbiotic nitrogen fixation. Our findings broadly support the general formulation of these carbon costs in the FUN biogeochemical model in response to shifts in nitrogen availability. However, there is a need for future studies to explicitly quantify carbon costs to acquire nitrogen under different environmental contexts, over longer temporal scales, and using larger selections of phylogenetically related species. In addition, we suggest that future studies minimize the limitations associated with the metric used here by explicitly measuring belowground carbon fates independently.

Chapter 3

Soil nitrogen availability modifies leaf nitrogen economies in mature temperate deciduous forests: a direct test of photosynthetic least-cost theory

3.1 Introduction

Photosynthesis represents the largest carbon flux between the atmosphere and land surface (**?**), and plays a central role in biogeochemical cycling at multiple spatial and temporal scales (**?**; **?**; **?**; **?**). Therefore, carbon and energy fluxes simulated by terrestrial biosphere models are sensitive to the formulation of photosynthetic processes (**?**; **?**; **?**; **?**; **?**) and must be represented using robust, empirically tested processes (**?**; **?**). Current formulations of photosynthesis vary across terrestrial biosphere models (**?**; **?**), which causes variation in modeled ecosystem processes (**?**; **?**; **?**; **?**) and casts uncertainty in ability of these models to accurately predict terrestrial ecosystem responses and feedbacks to global change (**?**; **?**; **?**).

Terrestrial biosphere models commonly represent C3 photosynthesis through variants of the **?** biochemical model (**?**; **?**; **?**). This well-tested photosynthesis model estimates leaf-level carbon assimilation, or photosynthetic capacity, as a function of the maximum rate of Ribulose-1,5-bisphosphate carboxylase-oxygenase (Rubisco) carboxylation (V_{cmax}) and the maximum rate of Ribulose-1,5-bisphosphate (RuBP) regeneration (J_{max}; Farquhar et al., 1980). Many terrestrial biosphere models predict these model inputs based on plant functional group specific linear relationships between leaf nutrient content and (V_{cmax}) (**?**; **?**; **?**) under the tenet that a large fraction of leaf nutrients, and nitrogen (N)

in particular, are partitioned toward building and maintaining enzymes that support photosynthetic capacity, such as Rubisco (**?**; **?**; **?**; **?**; **?**). Terrestrial biosphere models also predict leaf nutrient content from soil nutrient availability based on the assumption that increasing soil nutrients generally increases leaf nutrients (**?**)

3.2 Methods

3.3 Results

Chapter 4

Conclusions

References

Ainsworth, E. A. and S. P. Long (2005). What have we learned from 15 years of free-air CO2 enrichment (FACE)? A meta-analytic review of the responses of photosynthesis, canopy properties and plant production to rising CO2. *New Phytologist 165*(2), 351–372.

Allen, K., J. B. Fisher, R. P. Phillips, J. S. Powers, and E. R. Brzostek (2020). Modeling the carbon cost of plant nitrogen and phosphorus uptake across temperate and tropical forests. *Frontiers in Forests and Global Change 3*(May), 1–12.

Andersen, M. K., H. Hauggaard-Nielsen, P. Ambus, and E. S. Jensen (2005, jan). Biomass production, symbiotic nitrogen fixation and inorganic N use in dual and tri-component annual intercrops. *Plant and Soil 266*(1-2), 273–287.

Arndal, M. F., A. Tolver, K. S. Larsen, C. Beier, and I. K. Schmidt (2018). Fine root growth and vertical distribution in eesponse to elevated CO2, warming and drought in a mixed heathland–grassland. *Ecosystems 21*(1), 15–30.

Bates, D., M. Mächler, B. Bolker, and S. Walker (2015). Fitting linear mixed-effects models using lme4. *Journal of Statistical Software 67*(1), 1–48.

Bengtson, P., J. Barker, and S. J. Grayston (2012, aug). Evidence of a strong coupling between root exudation, C and N availability, and stimulated SOM decomposition caused by rhizosphere priming effects. *Ecology and Evolution 2*(8), 1843–1852.

Bloom, A. J., F. S. Chapin, and H. A. Mooney (1985, nov). Resource Limitation in Plants-An Economic Analogy. *Annual Review of Ecology and Systematics 16*(1), 363–392.

Bonan, G. B., M. D. Hartman, W. J. Parton, and W. R. Wieder (2013, mar). Evaluating litter decomposition in earth system models with long-term litterbag experiments: an example using the Community Land Model version 4 (CLM4). *Global Change Biology 19*(3), 957–974.

Bonan, G. B., P. J. Lawrence, K. W. Oleson, S. Levis, M. Jung, M. Reichstein, D. M. Lawrence, and S. C. Swenson (2011, may). Improving canopy processes in the Community Land Model version 4 (CLM4) using global flux fields empirically inferred from FLUXNET data. *Journal of Geophysical Research 116*(G2), G02014.

Booth, B. B. B., C. D. Jones, M. Collins, I. J. Totterdell, P. M. Cox, S. Sitch, C. Huntingford, R. A. Betts, G. R. Harris, and J. Lloyd (2012, jun). High sensitivity of future global warming to land carbon cycle processes. *Environmental Research Letters 7*(2), 024002.

Brix, H. (1971). Effects of nitrogen fertilization on photosynthesis and respiration in Douglas fir. *Forest Science 17*(4), 407–414.

Brzostek, E. R., J. B. Fisher, and R. P. Phillips (2014). Modeling the carbon cost of plant nitrogen acquisition: Mycorrhizal trade-offs and multipath resistance uptake improve predictions of retranslocation. *Journal of Geophysical Research: Biogeosciences 119*, 1684–1697.

Clark, D. B., L. M. Mercado, S. Sitch, C. D. Jones, N. Gedney, M. J. Best, M. Pryor, G. G. Rooney, R. L. H. Essery, E. Blyth, O. Boucher, R. J.

Harding, C. Huntingford, and P. M. Cox (2011, sep). The Joint UK Land Environment Simulator (JULES), model description – Part 2: Carbon fluxes and vegetation dynamics. *Geoscientific Model Development 4*(3), 701–722.

Cornwell, W. K., J. H. C. Cornelissen, K. Amatangelo, E. Dorrepaal, V. T. Eviner, O. Godoy, S. E. Hobbie, B. Hoorens, H. Kurokawa, N. Pérez-Harguindeguy, H. M. Quested, L. S. Santiago, D. A. Wardle, I. J. Wright, R. Aerts, S. D. Allison, P. van Bodegom, V. Brovkin, A. Chatain, T. V. Callaghan, S. Díaz, E. Garnier, D. E. Gurvich, E. Kazakou, J. A. Klein, J. Read, P. B. Reich, N. A. Soudzilovskaia, M. V. Vaieretti, and M. Westoby (2008, oct). Plant species traits are the predominant control on litter decomposition rates within biomes worldwide. *Ecology Letters 11*(10), 1065–1071.

Davies-Barnard, T., J. Meyerholt, S. Zaehle, P. Friedlingstein, V. Brovkin, Y. Fan, R. A. Fisher, C. D. Jones, H. Lee, D. Peano, B. Smith, D. Wårlind, and A. J. Wiltshire (2020, oct). Nitrogen cycling in CMIP6 land surface models: progress and limitations. *Biogeosciences 17*(20), 5129–5148.

Delaire, M., E. Frak, M. Sigogne, B. Adam, F. Beaujard, and X. Le Roux (2005, feb). Sudden increase in atmospheric CO2 concentration reveals strong coupling between shoot carbon uptake and root nutrient uptake in young walnut trees. *Tree Physiology 25*(2), 229–235.

Dovrat, G., H. Bakhshian, T. Masci, and E. Sheffer (2020, jul). The nitrogen economic spectrum of legume stoichiometry and fixation strategy. *New Phytologist 227*(2), 365–375.

Dovrat, G., T. Masci, H. Bakhshian, E. Mayzlish Gati, S. Golan, and E. Sheffer

(2018, jul). Drought-adapted plants dramatically downregulate dinitrogen fixation: Evidences from Mediterranean legume shrubs. *Journal of Ecology 106*(4), 1534–1544.

Evans, J. R. and J. R. Seemann (1989). The allocation of protein nitrogen in the photosynthetic apparatus: costs, consequences, and control. *Photosynthesis 8*, 183–205.

Exbrayat, J.-F., A. A. Bloom, P. Falloon, A. Ito, T. L. Smallman, and M. Williams (2018). Reliability ensemble averaging of 21st century projections of terrestrial net primary productivity reduces global and regional uncertainties. *Earth System Dynamics 9*(1), 153–165.

Farquhar, G. D., S. von Caemmerer, and J. A. Berry (1980, jun). A biochemical model of photosynthetic CO2 assimilation in leaves of C3 species. *Planta 149*(1), 78–90.

Firn, J., J. M. McGree, E. Harvey, H. Flores-Moreno, M. Schütz, Y. M. Buckley, E. T. Borer, E. W. Seabloom, K. J. La Pierre, A. M. MacDougall, S. M. Prober, C. J. Stevens, L. L. Sullivan, E. Porter, E. Ladouceur, C. Allen, K. H. Moromizato, J. W. Morgan, W. S. Harpole, Y. Hautier, N. Eisenhauer, J. P. Wright, P. B. Adler, C. A. Arnillas, J. D. Bakker, L. Biederman, A. A. D. Broadbent, C. S. Brown, M. N. Bugalho, M. C. Caldeira, E. E. Cleland, A. Ebeling, P. A. Fay, N. Hagenah, A. R. Kleinhesselink, R. Mitchell, J. L. Moore, C. Nogueira, P. L. Peri, C. Roscher, M. D. Smith, P. D. Wragg, and A. C. Risch (2019, feb). Leaf nutrients, not specific leaf area, are consistent indicators of elevated nutrient inputs. *Nature Ecology Evolution 3*(3), 400–406.

497 Fisher, J. B., S. Sitch, Y. Malhi, R. A. Fisher, C. Huntingford, and S.-Y. Tan
498 (2010). Carbon cost of plant nitrogen acquisition: A mechanistic, globally
499 applicable model of plant nitrogen uptake, retranslocation, and fixation.
500 *Global Biogeochemical Cycles 24*(1), 1–17.

501 Fox, J. and S. Weisberg (2019). *An R companion to applied regression* (Third
502 edit ed.). Thousand Oaks, California: Sage.

503 Franklin, O., R. E. McMurtrie, C. M. Iversen, K. Y. Crous, A. C. Finzi, D. Tis-
504 sue, D. S. Ellsworth, R. Oren, and R. J. Norby (2009, jan). Forest fine-root
505 production and nitrogen use under elevated CO₂: contrast-
506 ing responses in evergreen and deciduous trees explained by a common prin-
507 ciple. *Global Change Biology 15*(1), 132–144.

508 Friedlingstein, P., M. Meinshausen, V. K. Arora, C. D. Jones, A. Anav, S. K.
509 Liddicoat, and R. Knutti (2014). Uncertainties in CMIP5 climate projections
510 due to carbon cycle feedbacks. *Journal of Climate 27*(2), 511–526.

511 Friel, C. A. and M. L. Friesen (2019, nov). Legumes modulate allocation to
512 rhizobial nitrogen fixation in response to factorial light and nitrogen manip-
513 ulation. *Frontiers in Plant Science 10*, 1316.

514 Fujikake, H., A. Yamazaki, N. Ohtake, K. Sueoshi, S. Matsuhashi, T. Ito,
515 C. Mizuniwa, T. Kume, S. Hoshimoto, N.-S. Ishioka, S. Watanabe, A. Osa,
516 T. Sekine, H. Uchida, A. Tsuji, and T. Ohyama (2003, may). Quick
517 and reversible inhibition of soybean root nodule growth by nitrate in-
518 volves a decrease in sucrose supply to nodules. *Journal of Experimental*
519 *Botany 54*(386), 1379–1388.

520 Giardina, C. P., M. D. Coleman, J. E. Hancock, J. S. King, E. A. Lilleskov,

W. M. Loya, K. S. Pregitzer, M. G. Ryan, and C. C. Trettin (2005). The response of belowground carbon allocation in forests to global change. In D. Binkley and O. Manyailo (Eds.), *Tree Species Effects on Soils: Implications for Global Change* (Volume 55 ed.)., Chapter Chapter 7, pp. 119–154. Berlin/Heidelberg: Springer-Verlag.

Gibson, A. H. and J. E. Harper (1985, may). Nitrate effect on nodulation of soybean by Bradyrhizobium japonicum. *Crop Science 25*(3), 497–501.

Gill, A. L. and A. C. Finzi (2016). Belowground carbon flux links biogeochemical cycles and resource-use efficiency at the global scale. *Ecology Letters 19*(12), 1419–1428.

Goll, D. S., V. Brovkin, B. R. Parida, C. H. Reick, J. Kattge, P. B. Reich, P. M. van Bodegom, and Ü. Niinemets (2012, mar). Nutrient limitation reduces land carbon uptake in simulations with a model of combined carbon, nitrogen and phosphorus cycling. *Biogeosciences Discussions 9*(3), 3173–3232.

Gulmon, S. L. and C. C. Chu (1981, may). The effects of light and nitrogen on photosynthesis, leaf characteristics, and dry matter allocation in the chaparral shrub, Diplacus aurantiacus. *Oecologia 49*(2), 207–212.

Gutschick, V. P. (1981, nov). Evolved strategies in nitrogen acquisition by plants. *The American Naturalist 118*(5), 607–637.

Henneron, L., P. Kardol, D. A. Wardle, C. Cros, and S. Fontaine (2020, nov). Rhizosphere control of soil nitrogen cycling: a key component of plant economic strategies. *New Phytologist 228*(4), 1269–1282.

Hoagland, D. R. and D. I. Arnon (1950). The water-culture method for growing plants without soil. *California Agricultural Experiment Station: 347 347*(2), 1–32.

Hobbie, E. A. (2006, mar). Carbon allocation to ectomycorrhizal fungi correlates with belowground allocation in culture studies. *Ecology 87*(3), 563–569.

Hobbie, E. A. and J. E. Hobbie (2008, aug). Natural abundance of 15N in nitrogen-limited forests and tundra can estimate nitrogen cycling through mycorrhizal fungi: a review. *Ecosystems 11*(5), 815–830.

Hoek, T. A., K. Axelrod, T. Biancalani, E. A. Yurtsev, J. Liu, and J. Gore (2016, aug). Resource availability modulates the cooperative and competitive nature of a microbial cross-feeding mutualism. *PLOS Biology 14*(8), e1002540.

Högberg, M. N., M. J. I. Briones, S. G. Keel, D. B. Metcalfe, C. Campbell, A. J. Midwood, B. Thornton, V. Hurry, S. Linder, T. Näsholm, and P. Högberg (2010, jul). Quantification of effects of season and nitrogen supply on tree below-ground carbon transfer to ectomycorrhizal fungi and other soil organisms in a boreal pine forest. *New Phytologist 187*(2), 485–493.

Högberg, P., M. N. Högberg, S. G. Göttlicher, N. R. Betson, S. G. Keel, D. B. Metcalfe, C. Campbell, A. Schindlbacher, V. Hurry, T. Lundmark, S. Linder, and T. Näsholm (2008, jan). High temporal resolution tracing of photosynthate carbon from the tree canopy to forest soil microorganisms. *New Phytologist 177*(1), 220–228.

Houlton, B. Z., Y.-P. Wang, P. M. Vitousek, and C. B. Field (2008, jul). A unifying framework for dinitrogen fixation in the terrestrial biosphere. *Na-*

ture 454(7202), 327–330.

IPCC (2013). Climate Change 2013: The Physical Science Basis. Contribution of Working Group I to the Fifth Assessment Report of the Intergovernmental Panel on Climate Change. Technical report.

Johnson, N. C., J. H. Graham, and F. A. Smith (1997, apr). Functioning of mycorrhizal associations along the mutualism-parasitism continuum. *New Phytologist 135*(4), 575–585.

Kaiser, C., M. R. Kilburn, P. L. Clode, L. Fuchslueger, M. Koranda, J. B. Cliff, Z. M. Solaiman, and D. V. Murphy (2015, mar). Exploring the transfer of recent plant photosynthates to soil microbes: mycorrhizal pathway vs direct root exudation. *New Phytologist 205*(4), 1537–1551.

Kattge, J., W. Knorr, T. Raddatz, and C. Wirth (2009). Quantifying photosynthetic capacity and its relationship to leaf nitrogen content for global-scale terrestrial biosphere models. *Global Change Biology 15*(4), 976–991.

Kayler, Z., A. Gessler, and N. Buchmann (2010, sep). What is the speed of link between aboveground and belowground processes? *New Phytologist 187*(4), 885–888.

Kayler, Z., C. Keitel, K. Jansen, and A. Gessler (2017, mar). Experimental evidence of two mechanisms coupling leaf-level C assimilation to rhizosphere CO₂ release. *Environmental and Experimental Botany 135*, 21–26.

Kenward, M. G. and J. H. Roger (1997, sep). Small sample inference for fixed effects from restricted maximum likelihood. *Biometrics 53*(3), 983.

592 Knorr, W. (2000, jun). Annual and interannual CO₂ exchanges
593 of the terrestrial biosphere: process-based simulations and uncertainties.
594 *Global Ecology and Biogeography 9*(3), 225–252.

595 Knorr, W. and M. Heimann (2001, mar). Uncertainties in global terrestrial bio-
596 sphere modeling: 1. A comprehensive sensitivity analysis with a new photo-
597 synthesis and energy balance scheme. *Global Biogeochemical Cycles 15*(1),
598 207–225.

599 Kulmatiski, A., P. B. Adler, J. M. Stark, and A. T. Tredennick (2017, mar).
600 Water and nitrogen uptake are better associated with resource availability
601 than root biomass. *Ecosphere 8*(3), e01738.

602 Lawrence, D. M., R. A. Fisher, C. D. Koven, K. W. Oleson, S. C. Swen-
603 son, G. B. Bonan, N. Collier, B. Ghimire, L. Kampenhout, D. Kennedy,
604 E. Kluzek, P. J. Lawrence, F. Li, H. Li, D. L. Lombardozzi, W. J. Riley,
605 W. J. Sacks, M. Shi, M. Vertenstein, W. R. Wieder, C. Xu, A. A. Ali,
606 A. M. Badger, G. Bisht, M. Broeke, M. A. Brunke, S. P. Burns, J. Buzan,
607 M. Clark, A. Craig, K. M. Dahlin, B. Drewniak, J. B. Fisher, M. Flan-
608 ner, A. M. Fox, P. Gentine, F. M. Hoffman, G. Keppel-Aleks, R. Knox,
609 S. Kumar, J. Lenaerts, L. R. Leung, W. H. Lipscomb, Y. Lu, A. Pandey,
610 J. D. Pelletier, J. Perket, J. T. Randerson, D. M. Ricciuto, B. M. Sander-
611 son, A. Slater, Z. M. Subin, J. Tang, R. Q. Thomas, M. Val Martin, and
612 X. Zeng (2019, dec). The Community Land Model Version 5: description of
613 new features, benchmarking, and impact of forcing uncertainty. *Journal of*
614 *Advances in Modeling Earth Systems 11*(12), 4245–4287.

615 LeBauer, D. S. and K. Treseder (2008). Nitrogen limitation of net primary

productivity. *Ecology 89*(2), 371–379.

Lenth, R. (2019). emmeans: estimated marginal means, aka least-squares means.

Liang, J., X. Qi, L. Souza, and Y. Luo (2016, may). Processes regulating progressive nitrogen limitation under elevated carbon dioxide: a meta-analysis. *Biogeosciences 13*(9), 2689–2699.

Luo, Y., W. S. Currie, J. S. Dukes, A. C. Finzi, U. A. Hartwig, B. A. Hungate, R. E. McMurtrie, R. Oren, W. J. Parton, D. E. Pataki, R. M. Shaw, D. R. Zak, and C. B. Field (2004). Progressive nitrogen limitation of ecosystem responses to rising atmospheric carbon dioxide. *BioScience 54*(8), 731–739.

Markham, J. H. and C. Zekveld (2007, sep). Nitrogen fixation makes biomass allocation to roots independent of soil nitrogen supply. *Canadian Journal of Botany 85*(9), 787–793.

Matamala, R. and W. H. Schlesinger (2000, dec). Effects of elevated atmospheric CO₂ on fine root production and activity in an intact temperate forest ecosystem. *Global Change Biology 6*(8), 967–979.

Menge, D. N. L., S. A. Levin, and L. O. Hedin (2008, feb). Evolutionary tradeoffs can select against nitrogen fixation and thereby maintain nitrogen limitation. *Proceedings of the National Academy of Sciences 105*(5), 1573–1578.

Meyerholt, J., S. Zaehle, and M. J. Smith (2016, mar). Variability of projected terrestrial biosphere responses to elevated levels of atmospheric CO₂ due to uncertainty in biological nitrogen fixation. *Biogeosciences 13*(5), 1491–1518.

Muñoz, N., X. Qi, M. W. Li, M. Xie, Y. Gao, M. Y. Cheung, F. L. Wong, and H.-M. Lam (2016). Improvement in nitrogen fixation capacity could be part of the domestication process in soybean. *Heredity 117*(2), 84–93.

Nadelhoffer, K. J. and J. W. Raich (1992, aug). Fine root production estimates and belowground carbon allocation in forest ecosystems. *Ecology 73*(4), 1139–1147.

Norby, R. J., J. Ledford, C. D. Reilly, N. E. Miller, and E. G. O'Neill (2004, jun). Fine-root production dominates response of a deciduous forest to atmospheric CO2 enrichment. *Proceedings of the National Academy of Sciences 101*(26), 9689–9693.

Noyce, G. L., M. L. Kirwan, R. L. Rich, and J. P. Megonigal (2019). Asynchronous nitrogen supply and demand produce nonlinear plant allocation responses to warming and elevated CO₂. *Proceedings of the National Academy of Sciences 116*(43), 21623–21628.

Parvin, S., S. Uddin, S. Tausz-Posch, R. Armstrong, and M. Tausz (2020, jul). Carbon sink strength of nodules but not other organs modulates photosynthesis of faba bean (Vicia faba) grown under elevated [CO₂] and different water supply. *New Phytologist 227*(1), 132–145.

Phillips, R. P., E. R. Brzostek, and M. G. Midgley (2013). The mycorrhizal-associated nutrient economy: a new framework for predicting carbon-nutrient couplings in temperate forests. *New Phytologist 199*(1), 41–51.

Phillips, R. P., A. C. Finzi, and E. S. Bernhardt (2011, feb). Enhanced root exudation induces microbial feedbacks to N cycling in a pine forest under

long-term CO2 fumigation. *Ecology Letters 14*(2), 187–194.

Poorter, H., J. Bühler, D. Van Dusschoten, J. Climent, and J. A. Postma (2012). Pot size matters: A meta-analysis of the effects of rooting volume on plant growth. *Functional Plant Biology 39*(11), 839–850.

Prentice, I. C., X. Liang, B. E. Medlyn, and Y.-P. Wang (2015). Reliable, robust and realistic: The three R's of next-generation land-surface modelling. *Atmospheric Chemistry and Physics 15*, 5987–6005.

R Core Team (2021). R: A language and environment for statistical computing.

Raich, J. W., D. A. Clark, L. Schwendenmann, and T. E. Wood (2014, jun). Aboveground tree growth varies with belowground carbon allocation in a tropical rainforest environment. *PLoS ONE 9*(6), e100275.

Rastetter, E. B., P. M. Vitousek, C. B. Field, G. R. Shaver, D. Herbert, and G. I. Ågren (2001, jul). Resource optimization and symbiotic nitrogen fixation. *Ecosystems 4*(4), 369–388.

Rogers, A. (2014, feb). The use and misuse of V_{c,max} in Earth System Models. *Photosynthesis Research 119*(1-2), 15–29.

Rogers, A., B. E. Medlyn, J. S. Dukes, G. B. Bonan, S. Caemmerer, M. C. Dietze, J. Kattge, A. D. B. Leakey, L. M. Mercado, Ü. Niinemets, I. C. Prentice, S. P. Serbin, S. Sitch, D. A. Way, and S. Zaehle (2017, jan). A roadmap for improving the representation of photosynthesis in Earth system models. *New Phytologist 213*(1), 22–42.

Saleh, A. M., M. Abdel-Mawgoud, A. R. Hassan, T. H. Habeeb, R. S. Yehia, and H. AbdElgawad (2020, jun). Global metabolic changes induced by arbuscu-

lar mycorrhizal fungi in oregano plants grown under ambient and elevated levels of atmospheric CO₂. *Plant Physiology and Biochemistry 151*, 255–263.

Schaefer, K., C. R. Schwalm, C. Williams, M. A. Arain, A. Barr, J. M. Chen, K. J. Davis, D. Dimitrov, T. W. Hilton, D. Y. Hollinger, E. Humphreys, B. Poulter, B. M. Raczka, A. D. Richardson, A. Sahoo, P. Thornton, R. Vargas, H. Verbeeck, R. Anderson, I. Baker, T. A. Black, P. Bolstad, J. Chen, P. S. Curtis, A. R. Desai, M. C. Dietze, D. Dragoni, C. M. Gough, R. F. Grant, L. Gu, A. K. Jain, C. Kucharik, B. E. Law, S. Liu, E. Lokipitiya, H. A. Margolis, R. Matamala, J. H. McCaughey, R. Monson, J. W. Munger, W. Oechel, C. Peng, D. T. Price, D. Ricciuto, W. J. Riley, N. Roulet, H. Tian, C. Tonitto, M. Torn, E. Weng, and X. Zhou (2012, sep). A model-data comparison of gross primary productivity: Results from the North American Carbon Program site synthesis. *Journal of Geophysical Research: Biogeosciences 117*(G3), G03010.

Shi, M., J. B. Fisher, E. R. Brzostek, and R. P. Phillips (2016). Carbon cost of plant nitrogen acquisition: Global carbon cycle impact from an improved plant nitrogen cycle in the Community Land Model. *Global Change Biology 22*(3), 1299–1314.

Shi, M., J. B. Fisher, R. P. Phillips, and E. R. Brzostek (2019, jan). Neglecting plant–microbe symbioses leads to underestimation of modeled climate impacts. *Biogeosciences 16*(2), 457–465.

Smith, N. G. and J. S. Dukes (2013, jan). Plant respiration and photosynthesis in global-scale models: incorporating acclimation to temperature and CO

2. *Global Change Biology 19*(1), 45–63.

Smith, N. G., D. L. Lombardozzi, A. Tawfik, G. B. Bonan, and J. S. Dukes (2017, mar). Biophysical consequences of photosynthetic temperature acclimation for climate. *Journal of Advances in Modeling Earth Systems 9*(1), 536–547.

Smith, N. G., S. L. Malyshev, E. Shevliakova, J. Kattge, and J. S. Dukes (2016, apr). Foliar temperature acclimation reduces simulated carbon sensitivity to climate. *Nature Climate Change 6*(4), 407–411.

Soudzilovskaia, N. A., J. C. Douma, A. A. Akhmetzhanova, P. M. van Bodegom, W. K. Cornwell, E. J. Moens, K. K. Treseder, and J. H. C. Cornelissen (2015). Global patterns of plant root colonization intensity by mycorrhizal fungi explained by climate and soil chemistry. *Global Ecology and Biogeography 24*(3), 371–382.

Sulman, B. N., E. Shevliakova, E. R. Brzostek, S. N. Kivlin, S. L. Malyshev, D. N. L. Menge, and X. Zhang (2019). Diverse mycorrhizal associations enhance terrestrial C storage in a global model. *Global Biogeochemical Cycles 33*(4), 501–523.

Taylor, B. N. and D. N. L. Menge (2018, sep). Light regulates tropical symbiotic nitrogen fixation more strongly than soil nitrogen. *Nature Plants 4*(9), 655–661.

Terrer, C., S. Vicca, B. D. Stocker, B. A. Hungate, R. P. Phillips, P. B. Reich, A. C. Finzi, and I. C. Prentice (2018, jan). Ecosystem responses to elevated <scp>CO</scp> ₂ governed by plant–soil interactions and the cost of nitrogen acquisition. *New Phytologist 217*(2), 507–522.

Thomas, R. Q., E. N. J. Brookshire, and S. Gerber (2015, may). Nitrogen limitation on land: how can it occur in Earth system models? *Global Change Biology 21*(5), 1777–1793.

Thomas, R. Q., S. Zaehle, P. H. Templer, and C. L. Goodale (2013, oct). Global patterns of nitrogen limitation: confronting two global biogeochemical models with observations. *Global Change Biology 19*(10), 2986–2998.

Thornton, P. E., J.-F. Lamarque, N. A. Rosenbloom, and N. M. Mahowald (2007, dec). Influence of carbon-nitrogen cycle coupling on land model response to CO₂ fertilization and climate variability. *Global Biogeochemical Cycles 21*(4), GB4018.

Tingey, D. T., D. L. Phillips, and M. G. Johnson (2000, jul). Elevated CO₂ and conifer roots: effects on growth, life span and turnover. *New Phytologist 147*(1), 87–103.

Uselman, S. M., R. G. Qualls, and R. B. Thomas (2000). Effects of increased atmospheric CO₂, temperature, and soil N availability on root exudation of dissolved organic carbon by a N-fixing tree (Robinia pseudoacacia L.). *Plant and Soil 222*, 191–202.

van Diepen, L. T. A., E. A. Lilleskov, K. S. Pregitzer, and R. M. Miller (2007, oct). Decline of arbuscular mycorrhizal fungi in northern hardwood forests exposed to chronic nitrogen additions. *New Phytologist 176*(1), 175–183.

Vitousek, P. M., K. Cassman, C. C. Cleveland, T. Crews, C. B. Field, N. B. Grimm, R. W. Howarth, R. Marino, L. Martinelli, E. B. Rastetter, and J. I. Sprent (2002). Towards an ecological understanding of biological nitrogen fixation. In *The Nitrogen Cycle at Regional to Global Scales*, pp. 1–45.

Dordrecht: Springer Netherlands.

Vitousek, P. M. and R. W. Howarth (1991). Nitrogen limitation on land and in sea: how can it occur? *Biogeochemistry 13*(2), 87–115.

Vitousek, P. M., S. Porder, B. Z. Houlton, and O. A. Chadwick (2010, jan). Terrestrial phosphorus limitation: mechanisms, implications, and nitrogen–phosphorus interactions. *Ecological Applications 20*(1), 5–15.

Walker, A. P., A. P. Beckerman, L. Gu, J. Kattge, L. A. Cernusak, T. F. Domingues, J. C. Scales, G. Wohlfahrt, S. D. Wullschleger, and F. I. Woodward (2014, aug). The relationship of leaf photosynthetic traits - Vcmax and Jmax - to leaf nitrogen, leaf phosphorus, and specific leaf area: a meta-analysis and modeling study. *Ecology and Evolution 4*(16), 3218–3235.

Wang, W., Y. Wang, G. Hoch, Z. Wang, and J. Gu (2018, apr). Linkage of root morphology to anatomy with increasing nitrogen availability in six temperate tree species. *Plant and Soil 425*(1-2), 189–200.

Wieder, W. R., C. C. Cleveland, W. K. Smith, and K. Todd-Brown (2015, jun). Future productivity and carbon storage limited by terrestrial nutrient availability. *Nature Geoscience 8*(6), 441–444.

Wieder, W. R., D. M. Lawrence, R. A. Fisher, G. B. Bonan, S. J. Cheng, C. L. Goodale, A. S. Grandy, C. D. Koven, D. L. Lombardozzi, K. W. Oleson, and R. Q. Thomas (2019, oct). Beyond static benchmarking: using experimental manipulations to evaluate land model assumptions. *Global Biogeochemical Cycles 33*(10), 1289–1309.

Xu-Ri and I. C. Prentice (2017, apr). Modelling the demand for new nitrogen

fixation by terrestrial ecosystems. *Biogeosciences 14*(7), 2003–2017.

Zaehle, S., S. Sitch, B. Smith, and F. Hatterman (2005, sep). Effects of parameter uncertainties on the modeling of terrestrial biosphere dynamics. *Global Biogeochemical Cycles 19*(3), GB3020.

Zhu, Q., W. J. Riley, J. Tang, N. Collier, F. M. Hoffman, X. Yang, and G. Bisht (2019). Representing nitrogen, phosphorus, and carbon interactions in the E3SM land model: development and global benchmarking. *Journal of Advances in Modeling Earth Systems 11*(7), 2238–2258.

Ziehn, T., J. Kattge, W. Knorr, and M. Scholze (2011, may). Improving the predictability of global CO2 assimilation rates under climate change. *Geophysical Research Letters 38*(10), L10404.